Effect of Aluminium Additions on the Deactivation of Zinc in NaCl Solution

S. Hamoum-Moussaoui[1,2,*], A. Benchettara[1] and F. Kellou[1]

[1]Laboratoire d'Electrochimie- Corrosion, Métallurgie et Chimie Minérale. Faculté de Chimie, USTHB, BP 32 El-Alia, Bab Ezzouar, Alger 16111, Algeria

[2]Laboratoire des Matériaux et Minéraux Composites. Faculté des Sciences de l'Ingénieur, Université M'hamed Bougara de Boumerdès, Boumerdes 35000, Algeria

*Corresponding author: Tel: +213 21 247950-64; 247311; E-mail: moussaoui_sa1@yahoo.fr

The effect of aluminium in small additions (0.2, 0.4, 0.6 and 0.8 wt %) as alloying element on the corrosion behaviour of pure zinc as sacrificial anode was investigated in an aerated 0.5M NaCl solution. The electrochemical studies of the rotating zinc disc and zinc-aluminium electrodes were performed by means of the following electrochemical methods *i.e.*, linear polarization resistance, potentiodynamic polarization, electrochemical impedance spectroscopy (EIS) and Evans diagrams. All the results showed a decrease in the corrosion current density value with increasing the percentage of Al in Zn indicating that there is an improvement of the alloys corrosion resistance with respect to the pure zinc. Besides, the highest Al composition (0.8 wt % in Al) deactivates the sacrificial zinc anode without passivates it.

Key Words: Zn-alloy, Cathodic protection, NaCl, Sacrificial anode.

INTRODUCTION

Iron and steel of buried pipe lines in maritime structures are exposed at a severe corrosion. To avoid this problem, cathodic protection with sacrificial anodes is generally used, in order to shift corrosion potential of the materials towards cathodic values and make them cathodically protected. Zinc remains the most widely adopted anode materiel for cathodic protection in the conductive environments[1-4], despite the existence of other metals such as aluminium and magnesium. It should be noted that these metals are well known for their application in high resistivity environments (underground pipelines)[5]. The zinc is used in the oil industry for protecting steel storage tanks from corrosion as well as in the protection of structures buried in the soil. It is also used as hot-dip coatings to protect iron and steel against corrosion.

It is well known that on the surface of zinc, in contact with aqueous solution or in atmospheric exposure, a thin layer of zinc oxide and hydroxide develops[6,7]. This is why the reproducibility of zinc electrochemical measurements (corrosion potential and corrosion current) depends on the preparation of the zinc surface[8] and on the experimental conditions (pH of the solution, oxygen concentration, hydrodynamics, *etc.*).

In this study, we have compared the corrosion behaviour of pure Zn and Zn-xAl (x = 0.2, 0.4, 0.6 and 0.8 wt %) alloys immersed in 0.5M NaCl aerated aqueous solution at 25 ºC in order to find the optimal composition of Al which deactivates the Zn electrode without passivates it. The comparative electrochemical tests were performed using electrochemical impedance spectroscopy (EIS), linear polarization resistance, the potentiodynamic polarization and the Evans diagrams.

EXPERIMENTAL

Electrode preparation: The Zn-Al alloys with different percentages of Al (0.2, 0.4, 0.6 and 0.8 wt %) were elaborated from Zn (Aldrich, 99.99 % purity) and Al (Aldrich, 99.99 % purity) which were melted in an induction furnace (CELES) under controlled argon atmosphere. The working electrodes were pure Zn and Zn-Al alloys disc of 5 mm diameter mounted on a rotating disc electrode (RDE) system. The rotation speed of the disc was set at 500 revolutions per minute (rpm) in order to control the diffusion rate of dissolved oxygen. The electrode was mechanically polished with wet abrasive paper of increasingly finer grit up to 1200 mesh, rinsed with acetone then with distilled water. After that, it was immediately transferred into the test solution.

Electrochemical cell and electrolyte: The experimental piece of equipment to draw the curves was traditional device with three electrodes. A working electrode (Zn, Zn-Al alloys), a saturated calomel electrode was used as a reference electrode ($Hg/Hg_2Cl_2/Cl^-$) and a platinum plaque (5 mm × 5 mm) was used as a counter-electrode. A cell with double wall in order to maintain at 25 ºC was used. The corrosive solution

(0.5M NaCl) was prepared from NaCl (Prolabo) and distilled water.

Experimental techniques: The current-potential and impedance response of RDE were recorded with a Potentio-stat-Galvanostat type PGP201 and PGZ301 (Voltalab Radiometer Analytical) piloted by Volta Master 4 Software. The potentiodynamic polarization curves were recorded by changing the electrode potential automatically from cathodic to anodic potential with a scan rate of 1 mV/s. Linear polarization (Rp) measurements were carried out by applying an over-voltage of ± 20 mV at E_{corr} with scan rate of 0.1 mV/s. The EIS response of the samples was recorded in the range of 100-100 mHz, at free potential. The anode-carbon steel coupling in 3 % NaCl solution by the Evans method was studied with the surface ratio 1/2.5. All these techniques were conducted after maintaining the working electrode at its free potential for 20 min, until the steady state was obtained.

X-Ray diffractometer (Panalytical XPert PRO MPD) was used to identify the various phases using a cobalt anode (λ = 1,789 Å). The surface states were observed with a scanning electronic microscope (SEM), LEO S440, coupled with an energy dispersive X-ray EDX analysis system.

RESULTS AND DISCUSSION

Characterization of the surface samples: XRD patterns of Zn and Zn-xAl alloys (x = 0.2, 0.4, 0.6 and 0.8 wt %) are presented on the Fig. 1. While comparing between the various spectra, there is a broadening of the peaks and a variation of their intensities according to the increase in the percentage of aluminium.
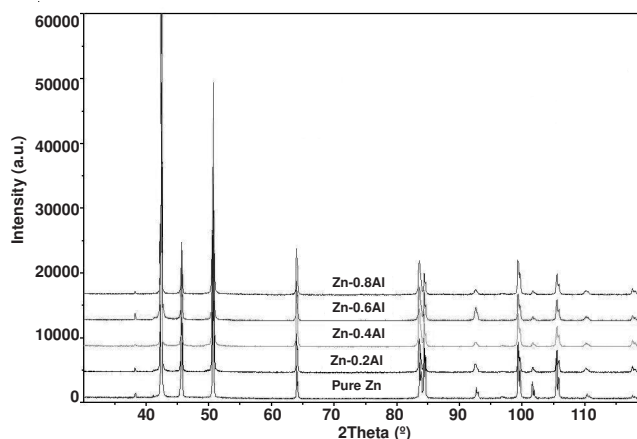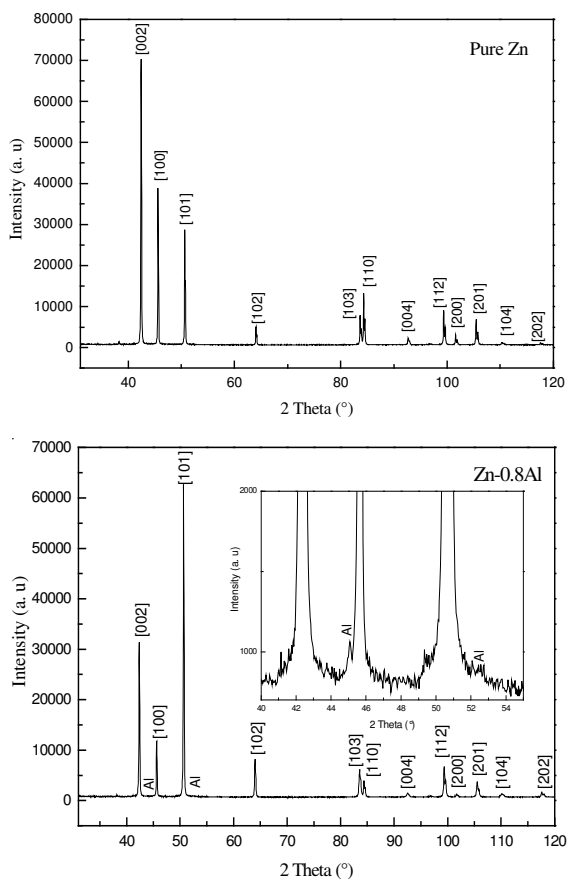
Fig. 1. XRD patterns of Zn and Zn-Al alloys

Aluminium enters the crystal lattice of zinc at the composition 0.2 wt % where the cell parameter decreases monotonically (Table-1) owing to the smaller radius of Al (1.18 Å) compared to that of Zn (1.25 Å). At x = 0.8 wt %, a mixed phase Zn0.98-Al0.2 (β-phase) coexists with α-phase rich in Al[9]. The detected second phase (α-phase) is well crystallized with a preferential orientation (111)[10].

TABLE-1
CRYSTALLOGRAPHIC PARAMETERS
OF Zn AND Zn-Al ALLOYS

Samples	Crystal system	a = b (Å)	c (Å)	α = β	γ
Zn	Hexagonal	2.66590	4.94610	90	120
Zn-0.2Al	Hexagonal	2.66493	4.95305	90	120
Zn-0.4Al	Hexagonal	2.66486	4.95331	90	120
Zn-0.6Al	Hexagonal	2.66486	4.95190	90	120
Zn-0.8Al	Hexagonal	2.66472	4.95299	90	120
	Cubic face centred	4.04940	4.04940	90	90

The SEM micrographs (Fig. 2) of a mechanical polished samples surface showed that the second phase (dark) starts to be formed in the alloy Zn-0.6Al wt % and that aluminium is distributed in this phase according to the energy dispersive X-ray (EDX) analysis carried out for the sample Zn-0.6Al wt %. For the other samples (Zn-0.2Al and Zn-0.4Al alloys) it is possible that α-phase is masked by matrix.
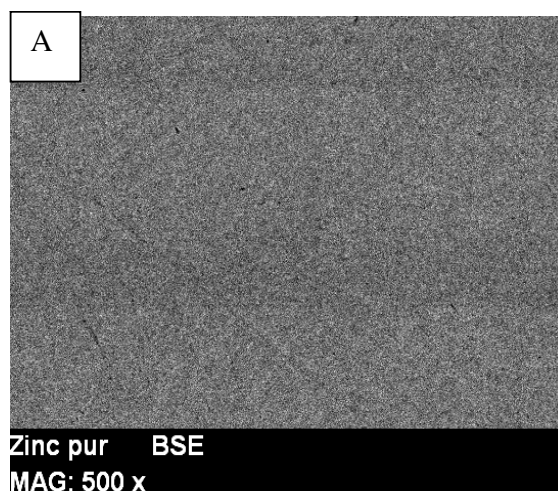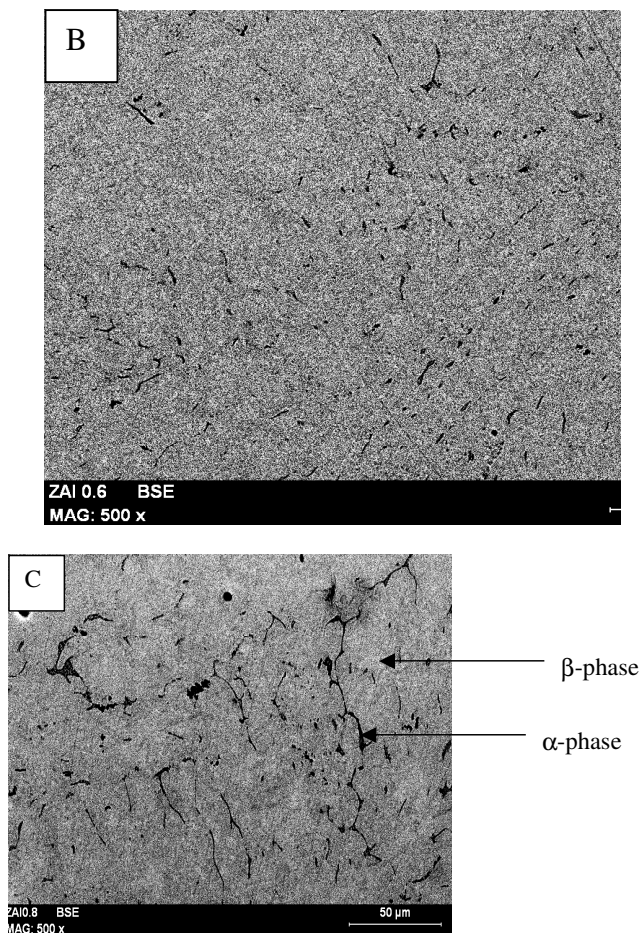
Fig. 2.   Representative SEM micrographs of pure Zn and Zn-Al alloys after polishing: (A) pure Zn; (B) Zn-0.6Al; and (C) Zn-0.8Al

Open circuit potential (OCP): The variation of open circuit potential of zinc and its alloys in aerated 0.5M NaCl, at 25 °C, according to immersion time of 20 min is presented in Fig. 3. The open circuit potential of all the studied samples is shifted towards more positive values until its stabilization, suggesting the formation of a corrosion products layer that slows down metal dissolution[11]. It is also noticed that the free potential becomes more negative when the percentage of aluminium increases.
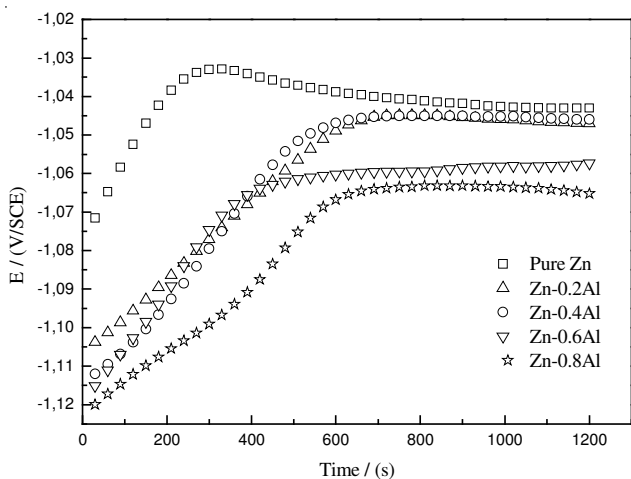
Fig. 3.   Variation of open circuit potential for zinc and zinc-aluminium alloys in aerated 0.5M NaCl solution, at 500 rpm, T = 25 °C

Potentiodynamic polarization curves: Fig. 4 shows the potentiodynamic polarization curves recorded for the rotating disc electrode of zinc and zinc-aluminium alloys in the studied solution. The cathodic branches of these curves exhibit two separated diffusion plateaux[12,13].
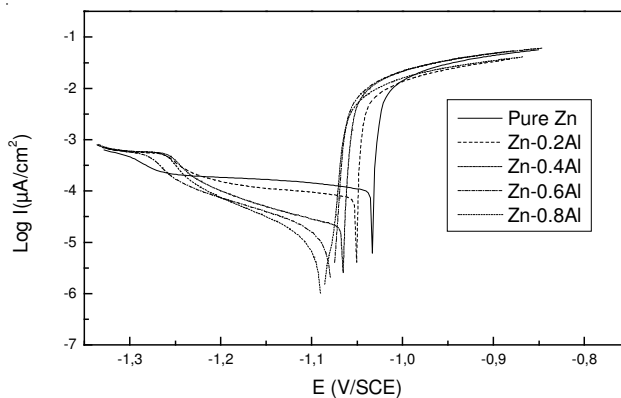
Fig. 4.   Polarization curves of zinc and zinc-aluminium alloys in aerated 0.5M NaCl solution at scan rate of 500 rpm, T = 25 °C

In order to separate the two cathodic processes a voltammogram (not presented here) was recorded on a bare surface of zinc and another on a surface covered by the oxide film formed after immersion of electrode for 20 min in the studied corrosive solution. The comparison between the two voltamograms shows a growth of the cathodic peak in the presence of the oxide. This observation can be explained by the formation of an electro reducible film on pure Zn. The results established more recently by Pilbath *et al.*[14], from the cyclic voltammograms and polarization curves of oxygen reduction on zinc disc electrode, show that the cathodic peaks of ZnO (de-aerated solutions) are superimposed on the oxygen reduction plateau. Besides it is reported in the literature[15-17] that the corrosion products formed on the surface of zinc are reduced at around -1.2 V. Thus, the plateau located at potentials lower than -1,23 V would correspond to the cathodic reduction of the film which is chemically formed during the immersion[18,19] and to the dissolved oxygen; the two corresponding reactions are presented below:

$$Zn(OH)_2 + 2e^- \rightarrow Zn + 2OH^- \qquad (1)$$

$$O_2 + 2H_2O + 4e^- \rightarrow 4OH^- \qquad (2)$$
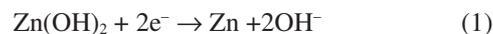
It can be noticed that the half-wave potential is constant and independent of the composition of the alloy. However, in the second plateau the cathodic reactional process depends of the alloy composition. The polarization curves of Zn and Zn-0.2Al wt % indicated that small amount of aluminium has not changed the cathodic branch shape. It is noted that the cathodic curves of other alloys showed a wider potential range of a mixed diffusion-activation control process at the plateau situated in the vicinity of E_{corr}. Therefore, the addition of Al to Zn from 0.4 wt % modifies the mechanism of oxygen reduction. It can be seen, that when the percentage of aluminium increased, the cathodic curves moved towards lower current values indicating that the surface exposed to the corrosive medium was less active.

One can see that the anodic current density increased according to the potential which corresponds to an extensive dissolution of the samples. Over a potential of -1 V, all the anodic curves were practically overlayed.

Linear polarization resistance: Polarization resistance Rp is defined as the slope of polarization curve at over potential of ± 20 mV/E_{corr}. We have then, recorded this curve for all the studied materials (not presented here) in 0.5 M NaCl solution.

It is a matter of fact that the corrosion current density i_{corr} is proportional to the value of Rp^{-1} according to Stern and Geary equation[20]:

$$i_{corr} = \frac{B}{Rp} \qquad (3)$$

The constant B can be calculated from the eqn. 4:

$$B = \frac{b_a b_c}{2.303(b_a + b_c)} \qquad (4)$$

b_a and b_c represent Tafel slopes of the anodic and cathodic portions respectively of the polarization curves.

As the value of $b_c \rightarrow \infty$,

then $\qquad i_{corr} = \frac{b_a}{2.303Rp} \qquad (5)$

The electrochemical parameters, of the studied samples in 3 % NaCl solution, obtained from polarization curves plots and linear polarization resistance method are given in Table-2. This includes: corrosion potential (E_{corr}), anodic Tafel slope (b_a), corrosion current density (i_{corr}), polarization resistance (Rp) and the constant (B).

As it can be seen from Table-2, the corrosion potential (E_{corr}) has slightly shifted towards the cathodic potentials. It can be observed that the corrosion current density (i_{corr}) decreases with the increase of Al percentage in pure Zn. It can be suggested the formation of a protective layer of aluminium and zinc hydroxides, acting as a barrier to oxygen diffusion, which reduces drastically the rate of cathodic reaction and therefore the corrosion current density of Zn-0.8Al in particular.

The obtained values of corrosion current density (i_{corr}) from the method of linear polarization resistance show the same trend with Tafel results. We can deduce that the presence of aluminium in the alloy slowed down the dissolution of the sacrificial anode, prolonging therefore its lifetime.

Analysis of electrochemical impedance spectroscopy: To discuss and correlate between the data obtained from the linear polarization resistance and those computed from potentiodynamic polarization technique we have used the electro-

chemical impedance spectroscopy (EIS) method. Electrochemical impedance spectroscopy is a valuable tool to study the degradation process in a corroding electrolyte and provides sensitive information on the diffusion behaviour of corroding systems. The impedance diagrams corresponding to zinc and its alloys in the corrosive medium are illustrated in Fig. 5.
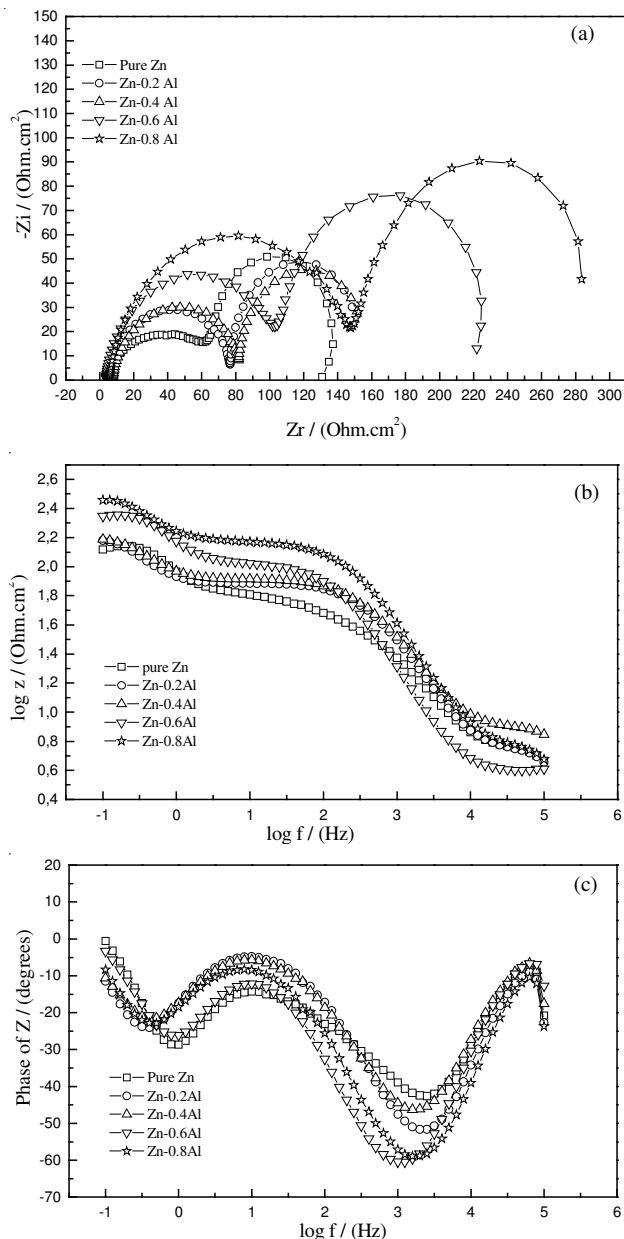
Fig. 5. Electrochemical impedance spectroscopy diagrams of zinc and zinc-aluminium alloys in 0.5M NaCl at scan rate of 500 rpm, T = 25 ºC; (a) Nyquist plots (b) Bode magnitude plots (c) Bode phase plots

TABLE-2
ELECTROCHEMICAL DATA OBTAINED FROM TAFEL METHOD AS WELL AS FROM LINEAR POLARIZATION
RESISTANCE CARRIED OUT IN AERATED 0.5M NaCl SOLUTION, FOR ZINC AND ZINC-ALUMINIUM ALLOYS

Samples	E_{corr} (mV/SCE)	Tafel method b_a (mV/dec)	i_{corr} (μA/cm^2)	Linear polarization resistance		
				Rp (Ωcm^2)	B (mV/dec)	i_{corr} (μA/cm^2)
Pure Zn	-1033	24.00	116.41	72.40	10.42	143.94
Zn–0.2Al	-1050	24.00	77.62	121.40	10.42	85.84
Zn-0.4Al	-1065	6.20	19.95	128.50	2.69	20.95
Zn-0.6Al	-1077	5.00	14.79	141.80	2.17	15.31
Zn-0.8Al	-1088	4.80	9.86	152.60	2.08	13.62

The Nyquist complex plane plot of the samples exhibits two capacitive loops. The high frequencies loop can be related to the charge transfer in combination with the accumulation of a corrosion product formed on the working electrode surface, whereas the second one is attributed to the diffusion process related mainly with the reduction of oxygen[18,21-23].

We remark that the addition of Al to Zn induces an increase of the circle diameter, indicating that the metallic dissolution is reduced. This change may be attributed to a decrease in the real surface of the specimen[24]. In the Bode diagrams, we can notice the presence of two time constants.

To simulate the electrochemical behaviour, an electrically equivalent circuit was proposed as model for the corrosion system on basis of the literature[13,21,25-31] and EIS characteristics:
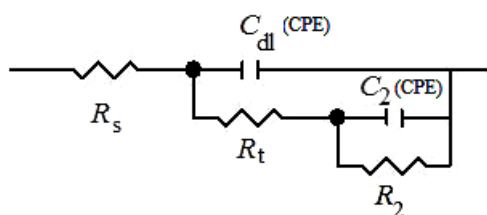
here, R_s represents the solution resistance, R_t and C_{dl} represent the charge transfer resistance and double layer capacitance associated with the corrosion process, R_2 and C_2 are the parameters related to the mass transport across the porous corrosion product layer. In addition, both C_{dl} and C_2 were replaced with constant phase element (CPE) in fitting procedure on consideration of the non-ideal capacitive response of he interface electrode/solution.

The electrochemical parameters deduced from the EIS technique are presented in Table-3.

The charge transfer resistance values (R_t) were calculated from the difference in impedance at the lower and higher frequencies, as suggested by Tsuru et al.[32]. To obtain the double layer capacitance (C_{dl}), the frequency (f) at which the imaginary component of impedance is maximum ($Z_{im\,max}$) was found and (C_{dl}) values were obtained from the equation:

$$f(-Z_{im})_{max} = \frac{1}{2\pi} C_{dl} R_t \qquad (6)$$

The E_{corr} measured (Table-3) for the different samples remain almost constant. However, there is an improvement of the charge transfer resistance which was observed for the alloys with respect to pure zinc. R_t increased with increasing the percentage in element addition, giving evidence of the better resistance corrosion of the alloys. The high double layer capacitance (C_2) obtained for the zinc is in good agreement

with the one observed by other authors in the case of zinc corrosion in aerated chloride or sulphate containing solution near neutral aqueous solutions and ascribed to the presence of porous layer of corrosion products[19,33]. The resistance R_2 was assumed to be related to the diffusion phenomenon, increases with increasing the percentage of Al in Zn.

Evans diagrams: We have studied the intrinsic behaviour of the sacrificial anode in 3 % NaCl solution by the curves I = f(E) and EIS method, whereas the behaviour of the galvanic-coupling anode with the structure to be protected was studied in 3 % NaCl solution by the Evans method. A comparison of the dissolution potentials of the different samples can lead to some aberrations[34]. Indeed, in present case, the Zn-0.8Al alloy whose dissolution potential is more electronegative (about -1088 mV) than that Zn which has a potential around -1033 mV, has a less reactive behaviour than Zn. Consequently, it is more efficient to measure the coupling current density, which gives the importance of galvanic corrosion.

The results obtained by Evans diagrams are shown in Figs. 6 and 7. From these results, one notices that the batteries function practically under cathodic control. The diagram of Zn alloy-steel shows a dual potential of -964.8 mV/SCE and a dissolution current density of 0.285 mA/cm² which indicates that this alloy is less reactive than pure Zn. Indeed, the application of Faraday's law gives for a current density of 0.285 mA/cm² (2,85 A/m²) an annual mass loss of 30.45 kg, whereas for a current density of 0.321 mA/cm² (Zn-steel) the annual mass loss is 34.29 kg. We have then succeeded in extending the life of our sacrificial anode by addition of 0.8 wt % Al.
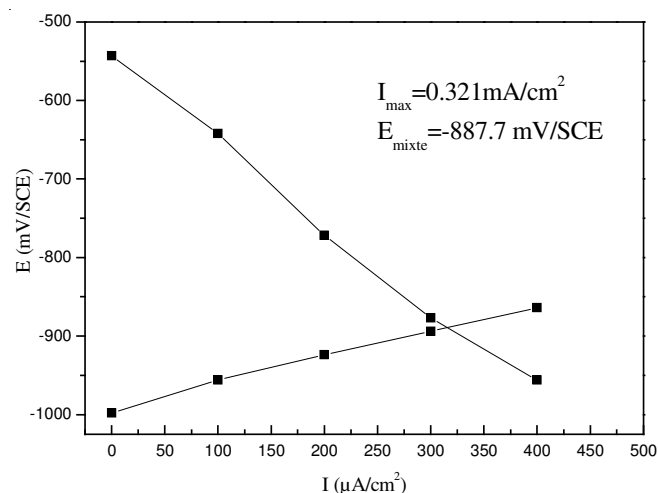
Fig. 6.　Evans diagram galvanic coupling of Zn⁻ carbon steel (surface ratio 1/2.5)

TABLE-3
ELECTROCHEMICAL DATA OBTAINED FROM EIS, IN AERATED 0.5M NaCl
SOLUTION, FOR ZINC AND ZINC-ALUMINIUM ALLOYS

Samples	1st loop			2nd loop	
	E_{corr} (mV/SCE)	1st loop R_t (Ωcm^2)	C_{dl} ($\mu F/cm^2$)	R_2 (Ωcm^2)	C_2 ($\mu F/cm^2$)
Pure Zn	-1040	46.55	8.55	68.80	3654
Zn-0.2Al	-1045	65.28	6.09	81.90	3110
Zn-0.4Al	-1047	79.74	6.31	82.05	3064
Zn-0.6Al	-1049	96.13	5.23	133.80	2377
Zn-0.8Al	-1052	142.90	4.45	198.90	1999
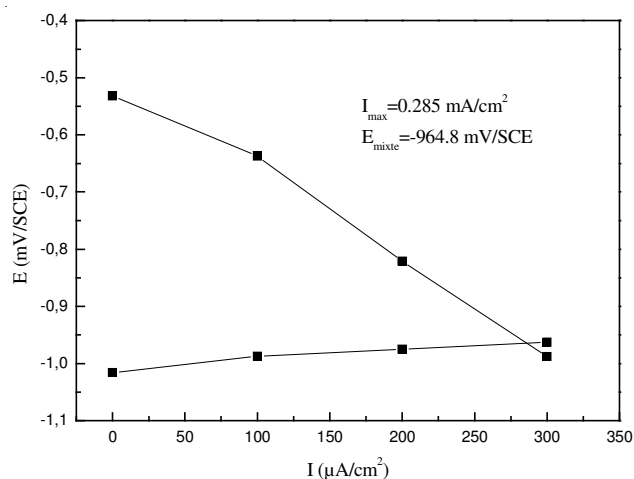
Fig. 7. Evans diagram galvanic coupling of Zn-0.8Al-carbon steel (surface ratio 1/2.5)

Conclusion

The addition effect of Al (0.2-0.8 wt %) on the dissolution rate of pure zinc was investigated in aerated aqueous sodium chloride (0.5 M) at 25 °C. The following points can be emphasized.

• The corrosion potentials for the samples tend towards more negative values according to an increase in the percentage of aluminium. In all cases, the potential was sufficiently low to allow as using these alloys as sacrificial anodes which can shift the mixed potential of the structure to be protected to immunity zone.

• All the electrochemical methods give the same results. In fact, all theses methods revealed that Zn-0.8 Al alloy has a good corrosion resistance, which gives anode a better lifespan with a good yield in the cathodic protection of immersed marine installations. Owing to the fact that the studied medium (sodium chloride solution) having NaCl content similar to that of natural sea water.

REFERENCES

1. M. Bounoughaz, E. Salhi, K. Benzine, E. Ghali and F. Dalard, *J. Mater. Sci.*, **38**, 1139 (2003).
2. D. Rabiot, F. Dalard, J.-J. Rameau, J.-P. Caire and S. Boyer, *J. Appl. Electrochem.*, **29**, 541 (1999).
3. A.R. Marder, *Prog. Mater. Sci.*, **45**, 191 (2000).
4. F.M. Androsch, K. Kosters and K.-H. Stellnberger, *Stahl Eisen*, **121**, 375 (2001).
5. I. Genesca, L. Betancourt, L. Jerade, C. Rodriguez and F.J. Rodriguez, *Mater. Sci.*, **289**, 1275 (1998).
6. M. Sagiyama, A. Hiraya and T. Watanabe, *J. Iron. Steel. Inst. (Japan)*, **77**, 244 (1991).
7. C.V. D'Alkaine and M.N. Boucherit, *Electrochem. J. Soc.*, **144**, 3331 (1997).
8. M.Y. Mourad, A.Y. Kandell and A.S. Elgaber, *Indian J. Technol.*, **28**, 612 (1990).
9. E.A. Brandes and G.B. Brook, Smithells Metals Reference Book, Oxford, edn. 7 (1992).
10. J.C.P.D.S. Card N° 04-0787.
11. S.C. Chung, A.S. Lin, J.R. Chang and H.C. Shih, *Corros. Sci.*, **42**, 1599 (2000).
12. A.P. Yadav, A. Nishikata and T. Tsuru, *Electroanal. Chem.*, **585**, 142 (2005).
13. S. Manov, A.M. Lamazouère and L. Ariès, *Corros. Sci.*, **42**, 1235 (2000).
14. Zs. Pilbath and L. Sziraki, *Electrochim. Acta*, **53**, 3218 (2008).
15. I. Suzuki, *Corros. Sci.*, **25**, 1029 (1985).
16. C. Allen, *Br. Corros. J.*, **26**, 93 (1991).
17. M. Pourbaix, Atlas of Electrochemical Equilibria in Aqueous Solutions, Pergamon Press, Oxford (1966).
18. C. Deslouis, M. Duprat and C. Tulet-Tournillon, *Electroanal. Chem.*, **181**, 119 (1984).
19. C. Deslouis, M. Duprat and C. Tournillon, *Corros. Sci.*, **29**, 13 (1989).
20. M. Stern and A.L. Geary, *J. Electrochem. Soc.*, **104**, 56 (1957).
21. M.C. Li, M. Royer and D. Stien, *Corros. Sci.*, **50**, 1975 (2008).
22. A.C. Bastos and M.G.S. Ferreira, *Prog. Org. Coat.*, **52**, 339 (2005).
23. V. Barranco, S. Feliu Jr. and S. Feliu, *Corros. Sci.*, **46**, 2203 (2004).
24. A. Barbucci, M. Delucchi and G. Cerisola, In Proceedings of the Fourth International Symposium on EIS, Rio de Janeiro, Brazil (1998).
25. T. Kosec, D.K. Merl and I. Milosev, *Corros. Sci.*, **50**, 1987 (2008).
26. M.C. Li, L.L. Jiang, W.Q. Zhang, Y.H. Qian, S.Z. Luo and J.N. Shen, *J. Solid. State Electrochem.*, **11**, 1319 (2007).
27. S. Magaino, M. Soga, K. Sobue, A. Kawaguchi, N. Ishida and H. Imai, *Electrochim. Acta*, **44**, 4307 (1999).
28. S.S.A. El-Rehim, H.H. Hassan and M.A. Amin, *Corros. Sci.*, **46**, 5 (2004).
29. F. Mansfeld, S. Lin, S. Kim and H. Shih, *Werkst Korros.*, **39**, 487 (1988).
30. F. Mansfeld, *Electrochim. Acta*, **38**, 1891 (1993).
31. C. Cao, *Corros. Sci.*, **38**, 2073 (1996).
32. T. Tsuru, S. Huruyama and B. Gjutsu, *J. Japan, Soc. Corros. Eng.*, **27**, 573 (1978).
33. L. Fedrizzi, L. Ciaghi, P.L. Bonoza, R. Fratesi and G. Roventi, *J. Appl. Electrochem.*, **22**, 297 (1992).
34. C. Vargel, Ingénieur Conseil en Corrosion de l'aluminium, Corrosion l'aluminium, Dunod (1998).